Research Journal of Chemical Sciences _____ ISSN 2231-606X
Vol. **5(2),** 23-31, February **(2015)** *Res. J. Chem. Sci.*

The Effect of Spinel formation in the Ceramic Welding Fluxes on the Properties of Molten Slag

Davidenko A. O.[1], Sokolsky V. E.[1]*, Lisnyak V. V.[1], Roik O. S.[1], Goncharov I. A.[2] and Galinich V. I.[2]
[1]Chemical Department, Taras Shevchenko National University of Kyiv, 01601 Kyiv, UKRAINE
[2]The E.O. Paton Electric Welding Institute, National Academy of Sciences of Ukraine, 03680 Kyiv, UKRAINE

Available online at: www.isca.in, www.isca.me
Received 11th January 2015, revised 28th January 2015, accepted 15th February 2015

Abstract

The magnesia- and alumina-based binary and ternary mixtures of the oxides as well as quaternary oxide-fluoride mixtures, which contain MgO and Al_2O_3, can form the spinel $MgAl_2O_4$ phase at high temperature treatment. The spinel phase formation and related issues were examined for these mixtures and commercial ceramic welding fluxes. Powder X-ray diffraction (PXRD), high temperature X-ray diffraction (HT-XRD), and gravimetry analysis were used to examine the phase composition of slags. For the major of the studied compositions, scanning electron microscopy (SEM) shows the formation of the prismatic microcrystallites of ca. 10-35 mkm. The energy dispersive X-ray (EDX) analysis confirms that pyramid-shaped prismatic crystals have $MgAl_2O_4$ spinel stoichiometry. The spinel crystallites are insoluble in the slags, according to the HT-XRD and PXRD data, and so the contribution of a part of the slag components that forming the spinel should be excluded at the estimation of characteristics of the slag melts. Based on this fact, it was proposed to quantify the spinel phase formed in the molten slag. Three convenient analytical techniques were proposed for the accurate determination of the weight and the volume fractions of the spinel phase in the slags. Two of these techniques are based on the internal standard method, which is applied in the framework of the quantitative PXRD analysis. The third technique is originated from the gravimetric analysis of the products of the solid slags etching that was conducted applying strong acids. The data obtained by the methods are sufficiently agrees with each other. The results of the spinel quantification were used to estimate the molten slag basicity and viscosity.

Keywords: Quantitative X-ray powder diffraction, internal standard method, molten slag, phase analysis, spinel, viscosity.

Introduction

The competitiveness of mechanic engineering products can be improved by the way of quality assurance. The latter could be realized, in particular, if obtain defect-free welded seams at substantial increase in the welding rate[1,2]. The perfect seams can be obtained at flux-cored arc welding (FCAW)[1]; if a weld pool damps fluctuations of the molten metal that are arisen at high welding rates. Therefore, the slag formed at the FCAW should characterized by gradual increase in viscosity at lowering the temperature[1-5]. In other words, FCAW needs for fluxes that support the formation of so-called long slags[2,3]. The latter are characterized by extended interval of the solidification[4,5]. However, large majority of fused fluxes[3-5], despite their fair-to-good technological properties, generate short slags. These slags are characterized by a sharp increase in the viscosity at lowering the temperature and cannot support the formation of high-quality welds at high-rate welding regime[4].

Ceramic (agglomerated) fluxes[5-7], which have found wide usage at the welding of high-strength and heavy-duty steels, are reasonable alternative to the fused fluxes[3,4]. These fluxes form long slags that can smooth the metal fluctuation inside the weld pool in a sufficiently wide range of temperatures. To improve a quality of welded seams one can use the alloying admixtures to FCAW wires[8]. Metallurgical aspects of FCAW were examined numerously for high strength low-alloying steels[1,2,9,10]. Thus, in the current literature there is scanty information on the structure of slag melts. The effect of the ceramic fluxes structure and composition on the physicochemical properties and technological characteristics of the molten slag is also beyond of the detail examination. In general, the structure of slag melts is described by several theories, which are of limited use as applied presumably to the equilibrium metallurgic process[11-13]. However, the welding, in most of the cases, belongs to non-equilibrium processes as being transient and is characterized by significant temperature gradients through a welding bath[7,11].

It is known, that at the FCAW the behavior of ceramic fluxes for substantially differs from that of the fused fluxes[1,4,7,13]. To ensure the lowest heat losses, the composition of the fused fluxes is usually designed to be close to the composition of the eutectic points in the multi-component systems[4,5]. In contrast to the ceramic fluxes, the fused fluxes are amorphous or semi-amorphous and do not melt at a certain temperature, thus over a certain range of temperatures. The wideness of this range determines their belonging to the short or long slag family[1,4,14]. The latter are better quenched oscillation of the weld pool metal as their characterized by high viscosity and density for a broader range of temperatures[14]. It should be noticed, that the

amorphisity of fused fluxes is caused by significant isothermal treatment of the slag melt at temperatures above the melting point and the granulation of the slag melt in the water or in the air flow[5].

In contrast to the fused fluxes, the ceramic fluxes are mainly consist of a mixture of crystalline components that melt gradually with temperature increasing[6,15]. For the period of FCAW, ceramic fluxes melt by parts and resulted molten slags can contain refractive crystalline solids within. At FCAW conditions, the ceramic fluxes form long slags due to the prolonged melting of the crystalline solids. At the first, a fusible part of these crystalline components melts at the lowest temperature. The rests of the crystalline components with higher melting points gradually melt with an increase of the temperature, while refractory components just only partially dissolve in the resulting molten slag. However, these molten slags can also contain other poorly soluble solids, such as crystals of $MgAl_2O_4$ spinel. The spinel is not the component of the initial ceramic flux, while is formed at the heating, if Al_2O_3 and MgO are the main constituent of the ceramic flux. The spinel is formed, according to our data[16,17], at the temperature range of 700–800 °C. The melting temperature of spinel is above 2000 °C, so heterogeneous slag, which is contain the oxide melt and dispersed microcrystals of the spinel, should possess increased viscosity, which is depend on the quantitative ratio between the molten mass and the mass of spinel crystals. It should emphasized that the spinel crystals grow at temperatures of 1420–1460 °C by parabolic law[18] and the can dissolved in the $CaO–SiO_2–Al_2O_3$ slags at 1504 °C[19]. Even so, the greater viscosity and smaller fluidity of the molten slag is depended on the content of the spinel phase in the slag. In this case, the slag belongs to the long slags family and, according to the theory[20], supplies favorable conditions for the metal damping in the weld pool. It should be pay an attention to the one feature of the slag, which contains crystals of spinel. The oxides, which are the components of the molten slags, hardly react with the spinel and the same is true for the welded metal being in the molten state[17]. This situation requires the consideration in the light of the slag properties prediction. Formally, for the prediction of the basicity of slag melts, one should take into account the effect of all the sum of the molten slag components even that are spent for the spinel forming. In our opinion, the quantity of component that is not involved in the metal-slag or the slag-forming component interactions should be subtracted from the calculation of the interaction-dependent functions, such as basicity.

Viscous characteristics of the molten slag containing solid particles are of high practical importance[1,9,13,20]. The viscosity affects on melting of metal, which is subjected to welding, on the formation of defect-free weld seams and regulates the transport of particle inside the molten slag[1,9]. Among numerous physical models and semi-empirical equations are being used for forecasting the viscosities of liquids, the equations derived from the Einstein's model the most correctly predict the viscosity of two-phase mixtures containing solid particles in the liquid phase. In general, the Einstein's model can be applied for the case of two-phase molten slags[21]. However, the Einstein-type equations, according to Frenkel[22], are more suitable for prediction of the effective viscosity if the two-phase mixture contains solid spherical particles of low concentration. In this case, the inter-particles interactions are accepted to be weak or even taken off from the consideration. Otherwise, the effective viscosity of two-phase suspension (η/η_0) according to the general model, can be described by using the Einstein-Roscoe equation:

$$\eta/\eta_0 = (1 - \alpha f)^{-n} \quad (1)$$

Where f is the volume fraction of the suspended particles, α and n are constants. The equation is valid for two-phase molten slags concentrated by the spinel if one assumes that the spinel forms solid hemispherical particles.

Summarizing, if the concentration of solid particles (in wt. % or vol. %) is known, it can be solved a significant number of issues related to the simulation of the main physicochemical behavior of the molten slags that are used for the FCAW. Therefore, the present study is directed on the quantitative determination of the spinel phase in the molten slag. Different analytical approaches were developed for such purpose and it was made an attempt to relay the obtained results with characteristics of the molten slags.

Material and Methods

Materials and chemicals: A UV 309P flux with chemical composition of $CaF_2/(SiO_2+TiO_2)/(Al_2O_3+MnO)/(CaO+MgO)$ (18/22/28/24, in wt. %, respectively) was supplied by Böhler Schweisstechnik GmbH. The reagents with a nominal purity of 99.9% MgO, Al_2O_3, SiO_2, and WO_3 of analytical grade were supplied by Sigma-Aldrich. Reagents, $Al(NO_3)_3 \cdot 9H_2O$, fluoride CaF_2, $Mg(NO_3)_2 \cdot 6H_2O$, double-distilled water, 25 wt. % NH_4OH, 65 wt. % HNO_3, 48 wt. % HF are from Merck chemicals.

Preparation of spinel: Preparation of the $MgAl_2O_4$ spinel phase and examination of reactivity of oxide-fluoride slag constituents were performed as follows. The $MgAl_2O_4$ spinel was prepared by low-temperature synthesis[23] as follows. A mixture of nitrate aqueous solutions of $Al(NO_3)_3 \cdot 9H_2O$ and $Mg(NO_3)_2 \cdot 6H_2O$, taken in the relation of 3:1, was co-precipitate with ammonia and filtered. The obtained filtrate was washed with rinsed water to pH ≅ 8. The precipitation product is a wet gel, which drying gives a mixture of hydroxides. The hydroxides mixture was calcined for 3 h at 1000 °C to a constant mass. The resulted powder composed of the crystalline spinel phase was thoroughly mixed in an agate mortar.

Testing reactivity of ceramic flux constituents: Binary and ternary oxide mixtures and ternary and quaternary oxide-fluoride mixtures that are constituents of commercial ceramic flux of composition $Al_2O_3/MgO/SiO_2/CaF_2$ (30/25/20/25, in wt.

%, respectively) were tested to be able forming the spinel phase. Five mixtures that are different by the composition were prepared. The regents, which are taken in the wt. % ratio of MgO/Al_2O_3(60/40), $Al_2O_3/MgO/SiO_2$(37.5/25/37.5), MgO/Al_2O_3(60/40), $Al_2O_3/MgO/CaF_2$(37.5/25/37.5), and $Al_2O_3/MgO/SiO_2/CaF_2$ (33/22.3/22.3/22.3), were mixed and the mixtures are denoted future as samples from 1 to 5, respectively. As some of these mixtures potentially can form the $MgAl_2O_4$ spinel, so, all these mixtures were annealed at different temperatures. To imitate the commercial ceramic welding flux, up to 10 wt. % of liquid glass (sodium/potassium silicates solution) was added to the sample 3 as a binder and then resulted mixture was heated up to 1500 °C in Mo crucibles by induction heating. The samples from 1 to 5 were remelted and slags were obtained. These slags were quenched and subjected to a future examination.

Preparation of ceramic flux and slags: The ceramic fluxes were prepared as follows. MgO, Al_2O_3, SiO_2 and CaF_2 reagents were taken in the wt. % ratio of 26/20/28/22, 34/21/19/22, 26/19/28/22, and 9/23/42/22, then were carefully mixed and mentioned future as samples from 6 to 9, respectively. The resulted mixtures were bound with sodium-potassium silicate solutions (liquid glass) and granulated. The granulated powders were annealed at 873 K in a shaft furnace.

Characterization of solid and molten slags: The quenched slags that are sputtered with 3 nm thick layer of pure platinum were studied by scanning electron microscopy (SEM). The slag samples were examined by means of a Jeol JSM 7700 F electron microscope. The surface morphology was photographed, and the elemental composition of selected areas was determined by using energy dispersive X-ray (EDX) spectrometer (Oxford, Inca X stream-2). Viscosity of the molten slags was measured by using a high-temperature rotational viscometer under a flow of purified argon, which is used to protect the molten slag, the working substance and the torsion bar from reactive oxygen and nitrogen gases that are components of the atmosphere. An automatic DRON-3 diffractometer and a diffractometer that is constructed for the investigation of melts[24,25] were used for X-ray diffraction studies. The diffractometer constructed for the investigation of melts[25] allows the study of solid and liquid samples at temperatures up to 1700 °C. The X-ray diffractometers were operated with MoKα-radiation (λ = 0.71073 Å), which monochromatization is performed by deferential Zr-Y filters. The crystallographic software packages Powder Cell 3.2[26], Crystallography Open[27] and PDF-2[28] databases were used to simulate, to analyze and to interpret powder X-ray powder diffraction (PXRD) and high temperature X-ray diffraction (HT-XRD) data.

Determination of the spinel content: Quantitative powder X-ray powder diffraction (QPXRD) analysis was used to determine the content of crystalline $MgAl_2O_4$ spinel phase in the solid and molten slags. The spinel quantification was performed by the area under the diffraction peak, which corresponds to the spinel phase, with using the internal standard method. This special QPXRD analytic technique is applied as the diffraction intensity is affected by the average absorption coefficient of the sample. Therefore, it is required to find the coefficient dependence from the mixture composition or eliminate the influence of the absorption factor[29]. According to the internal standard method, the reference substance was added in a constant percentage, by mass, to tested sample and the PXRD patterns of these mixtures were recorded. A calibration graph was plotted from the dependence of the ratio of the integrated area (S) under the major diffraction peaks of the analyte and the reference ($S_{anal.}/S_{ref.}$) against the analyte mass fraction ($W_{anal.}$)[30]. The calibration graph is used future at the determination of the spinel content from the data of X-ray experiments.

In the present study, original analytic methodology of the spinel quantification is proposed. The QPXRD studies are conducted using monoclinic phase of WO_3 oxide of recognized analytical grade, as the internal standard, and the spinel $MgAl_2O_4$ phase obtained by the low-temperature synthesis. The mixtures of $WO_3/MgAl_2O_4$ with different ratio of 80/20, 60/40, 50/50, 40/60, and 20/80 (in wt. %), which is necessary for the calibration, were thoroughly mixed in an agate mortar prior to the QPXRD examination. The ratio of $S(MgAl_2O_4)/S(WO_3)$, where *S* is the integrated areas under the diffraction peaks, was calculated from experimental QPXRD data using the integrated area under the diffraction peaks for the spinel reflection (311) and triple pseudo-cubic (002), (020), and (200) reflections of WO_3. The theoretical ratio $S(MgAl_2O_4)/S(WO_3)$ was found from PXRD patterns of $MgAl_2O_4/WO_3$ mixtures simulated within the Powder cell 3.2 framework[26]. The measured and the simulated $S(MgAl_2O_4)/S(WO_3)$ ratios were plotted against the weight fraction of spinel, $W(MgAl_2O_4)$. These plots were used future as the calibration graphs.

The chemical etching method with subsequent gravimetric analysis of residues was elaborated for the spinel quantitative determination. According to the method, the solid slags were etched sequentially with 40 wt. % HF and then with the excess of 65 wt. % HNO_3 aqueous solution. The resulted fluoride-nitrate solution was filtered off and insoluble residues on a filter paper were first washed with hot double-distilled water and then dried. The dried solid residues were characterized by PXRD and SEM-EDX analyses and weighted on Mettler Toledo AE 100 analytical balance for the spinel quantification[31].

Results and Discussion

The spinel quantification by QPXRD analysis: Figure-1a-1b shows the experimental and simulated PXRD patterns of the initial components. As can be seen from the figure-1a-1b, the internal standard X-ray reflections are not overlap the main reflection assigned to the spinel phase. Figure-1c demonstrates the experimental PXRD patterns of $WO_3/MgAl_2O_4$ mixtures that normalized to the powder pattern of WO_3. Figure-1d shows the dependence of $S(MgAl_2O_4)/S(WO_3)$ against $W(MgAl_2O_4)$. The

calibration curves (1) and (2) were plotted from the data obtained from the experimental PXRD patterns and that simulated from respective crystallographic data, respectively. A good agreement between both curves is obtained at the low concentration of the $MgAl_2O_4$ spinel phase, up to 30 wt. %.

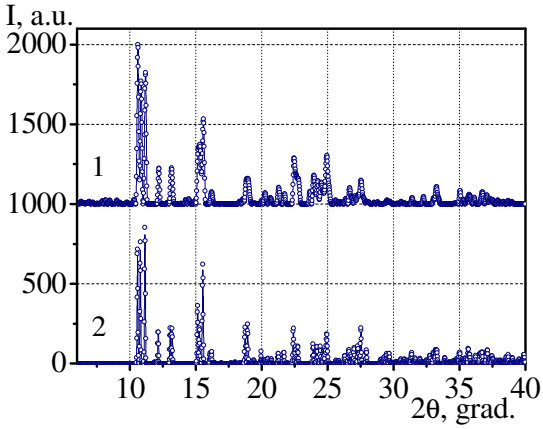

Figure-1A

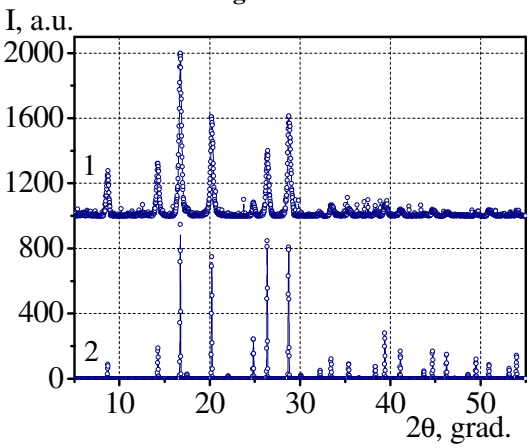

Figure-1B

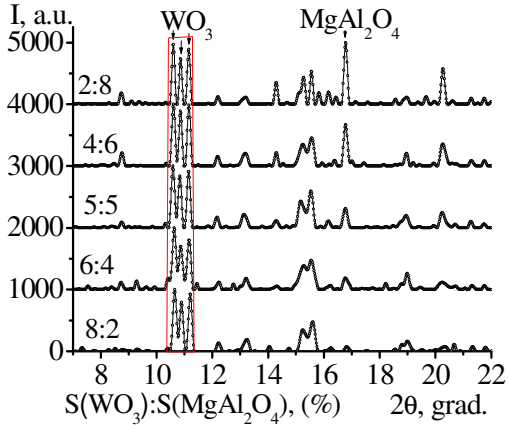

Figure-1C

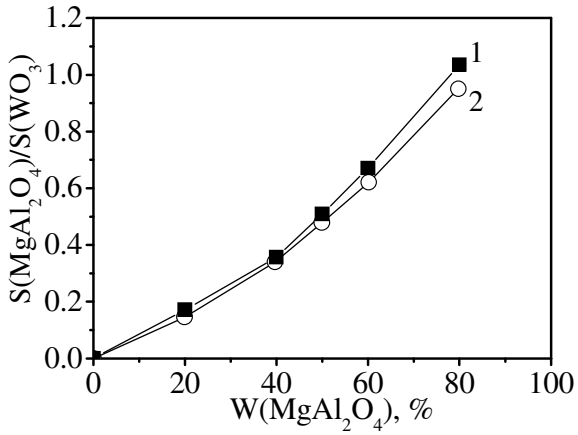

Figure-1D

Figure-1

Experimental (1) and simulated (2) PXRD patterns: (A) WO_3 and (B) $MgAl_2O_4$, (C) experimental PXRD patterns of mixtures with a known ratio of $WO_3/MgAl_2O_4$, (D) calibration graphs: (1) experimental ratio of $S(WO_3)/S(MgAl_2O_4)$ and (2) the ratio derived from the simulated PXRD patterns

In general, the internal standard method is a simple and precise analytical method[30], if the calibration graph of the $S(MgAl_2O_4)/S(WO_3)$ versus $W(MgAl_2O_4)$ is of a linear type. Hence, in our case, there is a certain deviation, which is also found for the dependence that is graphed from the simulated PXRD patterns. As the theoretical and experimental dependences coincide well, so instrumental errors are apparently small and we can assume that both methods are applicable in practice.

The internal standard method was tested on the commercial UV 309P flux. As in the previous measurements, up to 50 wt. % of WO_3 was added to the initial samples of the flux. All the obtained UV 309P/WO_3 mixtures were remelted for 30 min at temperatures in the range of 1200 °C–1500 °C, and then obtained molten slags were rapid quenched to r.t. The gravimetric analysis of the slags remelted at the stated temperatures shows that no lost of the weight is observed, so there is no evidence of WO_3 sublimation from the flux at such experimental conditions. However, we did not study temperatures above the temperature of the partial melting of the slag, since at the prolonged isothermal exposure, for periods longer than 30 min, a slight dissolution of WO_3 in the molten slag was observed. Figure-2a shows typical PXRD patterns of obtained UV 309P/WO_3 (50/50, in wt. %) solid slags, which are studied after isothermal exposures at high temperatures and rapid cooling. Figure-2b shows the temperature dependence of $W(MgAl_2O_4)$, which was determined from the data of QPXRD analysis of the solid UV 309P slags. It should be noticed that the quantity of spinel in the molten slag, which is remelted at 1500 °C, and the quantity of spinel in the solidified slag is almost the same, according to the quantitative analysis that is based on the HT-XRD and PXRD data. This is true for all the

investigated welding fluxes.

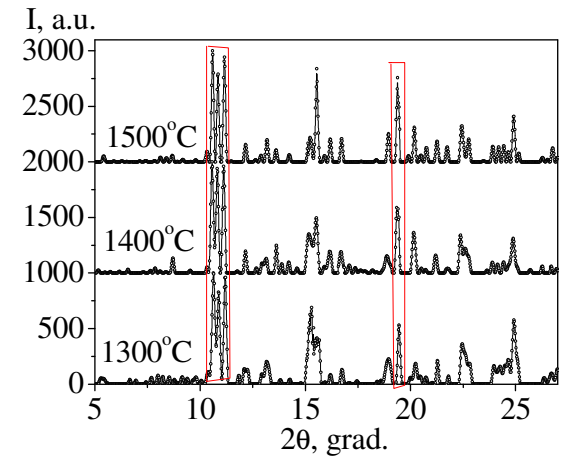

Figure-2A

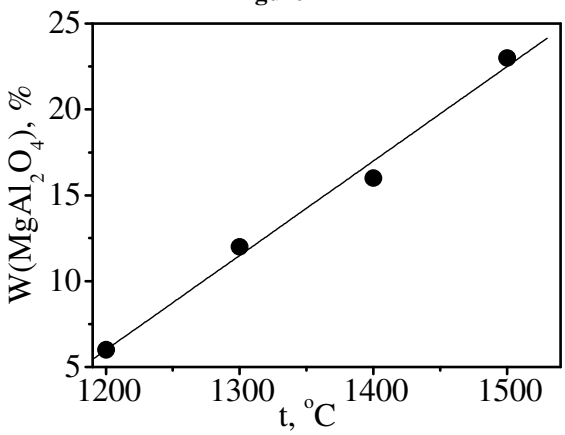

Figure-2B

Figure-2

(A) Representative PXRD pattern of quenched slags of the composition (UV 309P)+WO_3 (50/50, in wt. %) that are exposed at different temperatures, (B) The temperature dependence of the spinel content in the UV 309P slag from PXRD data

The spinel quantification by etching and subsequent gravimetric analysis: The spinel $MgAl_2O_4$ is a quite resistant to acidic medium and insoluble in the major of mineral acids, in contrast to other slags components[32]. So, the solid slag etching applying HF and HNO_3 causes sequentially dissolution of silica and then the rests of the oxide components. Figure-3 shows PXRD patterns of the solid residues obtained after different slags etching.

Registered PXRD patterns show mainly the spinel phase X-ray reflections and practically no reflections belonging to other crystalline phases were found. So, the gravimetric quantification method could be used to determine the spinel content in the slags.

Results of testing reactivity of ceramic flux constituents: In general, the most of slags studied form the spinel phase. Figure-4 shows typical SEM micropohoto of the solid slag obtained after remelting of the ceramic flux, sample 4, at 1500 °C.

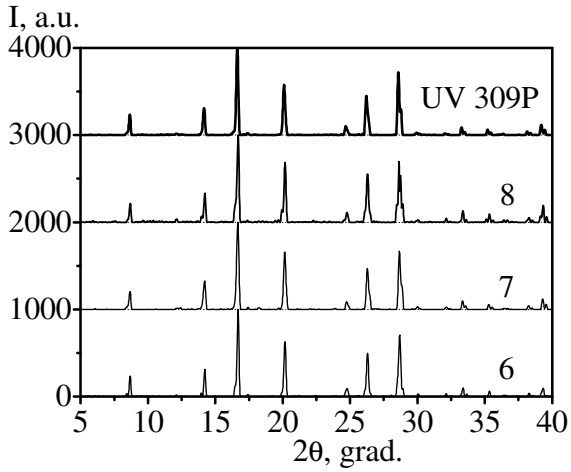

Figure-3

PXRD patterns of the solid residues obtained after slags etching, numbers corresponds to the numbering of the examined samples

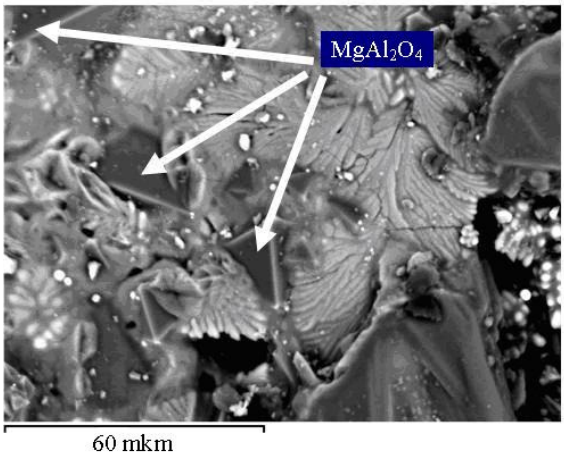

Figure-4

SEM microphoto of the solid slag obtained by remelting at 1500°C and quenching of the ceramic flux

SEM-EDX microanalysis showed that the pyramid dark crystals, marked with arrows, are of $MgAl_2O_4$ spinel stoichiometry. SEM-EDX of initial ceramic fluxes and obtained slags shows that the spinel crystallites are in a range from 10 to 35 mkm and are absent completely in the ceramic flux before remelting.

In the case of the samples 4 and 5, in a series of experiments (the samples from 1 to 5), the spinel is formed already at 1100 °C. However, the low-intensity reflections, such as from the spinel can be detected by the PXRD even at 800 °C, but their identification is complicated by the similarity in their 2θ

position with cubic phase of Al_2O_3. On the other hand, SEM-EDX studies confirm the presence of the spinel crystals in the solid slag. In all other cases, samples from 1 to 3, the spinel is formed at 1300 °C. This means that the presence of CaF_2 reduces the temperature of the spinel formation, as the product of high-temperature reactions between the components. The formation of spinel is affected by the CaF_2 content that is documented well elsewhere[33,34]. In general, an increase of the content of CaF_2 reduces the polymerization degree of the molten slag and, so, the critical temperature of melting is lowered[34]. The latter causes the concretion of the particles contained in the melt. The decrease in the critical temperature by about 150–200 °C is found for these molten slags[34]. At the same time, the addition to the flux of 10 mass.% of MgO increases the critical temperature on *c.a.* 100 °C. Addition of SiO_2 should complicate the formation of spinel in the molten slag, as it can react actively with SiO_2 and MgO, then these components between each other. Hence, we found no experimental confirmation of this fact. In contrast to data of Nikolaev et al.[35], we found no considerable effect of the liquid glass on the process that are realized at the molten slags[36]. The water from the ceramic flux completely evaporates at 200–250 °C. At higher temperatures, crystalline sodium silicates possibly destruct and silica dissolves in the molten slags. The inclusions enriched with sodium, according to SEM-EDX data, are concentrated on the surface of scorified slag, as seen from figure-5. The flotation of Na to the upper part of the molten slag causes formation of the Na-rich inclusions that are marked with arrows on the SEM micrograph in the solid slag. Here, also admixture quantities of S and P (up to 0.02 wt. %) was registered by EDX.

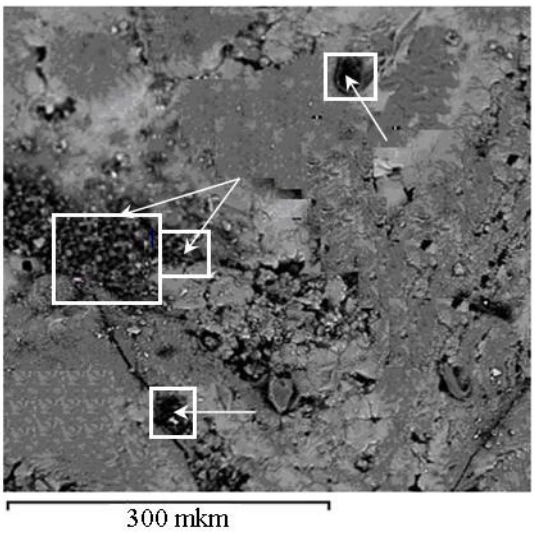

Figure-5
SEM microphotograph taken from the upper part of the slag obtained for the sample 6

These inclusions are completely absent in the slag volume, according to the SEM-EDX data collected for samples that are cut off for the slag bulk. It was shown in the literature[13] that the reactions run with participation of products of liquid glass (Na_2SiO_3) destruction result in the formation of perovskite ($CaTiO_3$) and sphene ($CaTiSiO_5$). Despite the fact that the sodium and sodium-potassium silicate glasses are regents that can participated in the stated reaction, the composition of the glass used in the present study is differ from that reported[34]. The composition of the liquid glasses used in the present study is closer to SiO_2-rich then to Na_2SiO_3-rich glasses. Summarizing the results of our studies, we found that no additional products of the liquid glass reaction with components of the molten slag are formed. Also, no products of the destruction of the liquid glass were found from PXRD and HT-XRD patterns. These observations confirm statements done on the base of SEM-EDX data. At the most probable scenario of the molten slag formation, the sodium silicate destructs at high temperatures, silica reacts with other molten slag components, while sodium oxide remains an inert component.

Table-1 shows the values of $W(MgAl_2O_4)$ for the slags, which was calculated from the data of QPXRD and etching (E). The initial weight percents of the ceramic flux components and the basicity (B) were also listed in the table-1. The values of basicity (B_1, B_2, and B_3) were calculated with or without accounting of the spinel formation by the formula:

$$B_n = W(MgO)/(W(SiO_2) + 0.5W(Al_2O_3)) \quad (2)$$

Where n is the lower index equals to 1, 2 or 3, W(MgO), $W(SiO_2)$, and $W(Al_2O_3)$ are the weight percents of reagents, B_2 is calculated from the same formula excluding the weight percents of reagents that form the spinel, B_3 value was calculated as B_2, however, the rests of the reagents that are not spent on the spinel formation were recalculated on 100 wt. %. As can be seen from the data of the table-1, the slag samples 6, 7, and 8 form the $MgAl_2O_4$ spinel, but the sample 9, taken for the comparison, does not contain the spinel phase. The values of B_1, B_2, and B_3, which are calculated with or without accounting of the spinel effect, are slightly different from each other. However, it should be expected that these values may differ significantly for other compositions.

The volume percents of the spinel, which are listed in the table-2, were corresponded to f values of the equation-1. The experimental η and the following parameters of $\alpha = 1.35$, $f = 0.3$ and $n = 2.5$ for the Einstein-Roscoe equation were used to prediction the molten slag viscosity, η_0. Figure-6 shows the experimental points, the smoothed value of η, and the calculated value of η_0. It should be noted that the dependence is quite similar to the smoothed experimental curve of viscosity, but the numerical values are smaller.

This is consistent, since the viscosity without inclusion of the spinel crystallites should possess lower temperature values. At the same time, the curve (2) should characterize by a sharp increase of the viscosity at cooling, which is known feature of the short slags. Hence, this feature does not occur because the fact that at 1100–1300 °C some of the flux components remain

in the solid state.

Table-1
The composition of ceramic fluxes, the spinel content (QPXRD and etching (E) data) and the basicity values

Sample No	Components, (W, wt. %)									Basicity, B	
	Al_2MgO_4		MgO	Al_2O_3	SiO_2	CaF_2	Na_2O	K_2O	Fe_2O_3		
	QPXRD	E									
6	-	-	26	20	28	22	2	1	2	B_1	0.68
	20	19	20	5	28	22	2	1	2	B_2	0.66
	-	-	25	6	35	28	3	1	2	B_3	0.68
7	-	-	34	21	19	22	2	0	1	B_1	1.18
	28	27	28	6	19	23	2	0	1	B_2	1.27
	-	-	35	8	24	29	3	0	1	B_3	1.25
8	-	-	26	19	28	22	2	1	2	B_1	0.69
	21	21	18	0	28	21	2	1	2	B_2	0.64
	-	-	25	0	39	29	3	1	3	B_3	0.64
9	-	-	9	23	42	22	2	1	1	B_1	0.21

Table-2
Shows the volume percents (V) of the components and the spinel that are recalculated from the QPXRD and etching data

Sample No	Components, (V, vol. %)							
	$AlMg_2O_4$	MgO	Al_2O_3	SiO_2	CaF_2	Na_2O	K_2O	Fe_2O_3
6	25	26	6	6	31	4	2	2
7	19	19	4	32	21	3	1	1
8	20	17	0	36	22	3	1	1
9	0	8	18	50	22	1	1	0

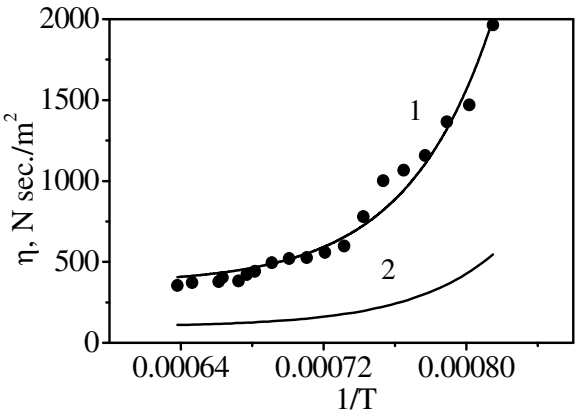

Figure-6
Temperature dependence of the viscosity for the slag sample 7, experimental data (points); smoothed data, curve (1); the predicted value of η_0 depicted by curve (2)

Conclusion

The mixtures of components of the ceramic fluxes for FCAW, which contain MgO and Al_2O_3, are formed the spinel $MgAl_2O_4$ crystallites at the heating. The spinel formation was confirmed by HT-XRD, QPXRD and SEM-EDX analysis. The $MgAl_2O_4$ spinel is insoluble in the molten slag, so the contribution of a part of the components that forming the spinel could be excluded at the estimation of the slag physicochemical characteristics. To determine the weight and volume fractions of the spinel phase in the solids obtained by quenching of the molten slags, convenient analytical methods that are based on the QPXRD and the gravimetric analyses were proposed. The results obtained by the methods are sufficiently agrees with each other. The attempts to accounting the effect of spinel phase to makes more correct the prediction of the molten slag viscosity and basicity were performed.

References

1. Minnick W.H., Flux Cored Arc Welding Handbook, Goodheart-Willcox, Tinley Park, IL, 176 **(2008)**

2. Pokhodnya I.K., Metallurgy of arc welding of structural steels and welding materials, *Welding International*, **24(11)**, 867-878 **(2010)**

3. Kobelco Welding Handbook 2014, Kobe steel LTD, Kobe, Japan, available online at: http://www.kobelco.co.jp/english/welding/handbook/pageview/html/category.html, (01.01.2015), **(2015)**

4. Podgaetskii V.V. and Kuzmenko V.G., Welding slag, Naukova Dumka, Kiev, 256 **(1988)**

5. Podgaetsky V.V. and Lyuborets I.I., Welding fluxes, Tekhnika, Kiev, 167 **(1984)**

6. Brook R.J., Concise encyclopedia of advanced ceramic materials, Pergamon, Oxford, 588 **(1991)**

7. Pokhodnya I.K., Gorpenyuk V.N., Milichenko S.S. and Ponomarev V.E., Metallurgy of arc welding: arc processes and electrode melting, Riecansky Science, Cambridge, UK, 250 **(1992)**

8. Sokolsky V.E., Roik O.S., Davidenko A.O., Kazimirov

V.P., Lisnyak V.V., Galinich V.I., Goncharov I.A. and Tokarev V.S., What makes a good weld in terms of its structure and chemical composition?**,** *Research journal of Chemical Sciences*, **4(12)**, 86-92 **(2014)**

9. Olson D.L., The investigation of the influence of welding flux on the pyrometallurgical, physical and mechanical behavior of weld metal, Final report of Center for welding research, Colorado school of mines, Golden, Colorado, 28 **(1983)**

10. Eagar T.W., Thermochemistry of joining, in Koros P.J. and St. Pierre G.R. (Eds.), Elliot Symp. on Chemical Process Metallurgy, Iron and Steel Society, Warrendale, 197-208 **(1991)**

11. Yakobashvili S.B., Surface properties of welding fluxes and slags, Tekhnika, Kiev, 208 **(1970)**

12. Novozhilov N.M., Fundamental metallurgy of gas-shielded arc welding, Gordon and Breach, New York, 400 **(1988)**

13. Boronenkov V., Zinigrad M., Leontiev L., Pastukhov E., Shalimov M. and Shanchurov S., Phase Interaction in the Metal–Oxide Melts–Gas System: The Modeling of Structure, Properties and Processes, Springer, New York-Berlin-Heidelberg, 410 **(2012)**

14. Deyev G.F. and Deyev D.G., Physical Chemistry of Fusion Welding, DGD Press, St. Paul, MI, 780 **(2009)**

15. Golovko V.V. and Potapov N.N., Special features of agglomerated (ceramic) fluxes in welding, *Welding International*, **25(11)**, 889-893 **(2011)**

16. Goncharov I.A., Sokolsky V.E., Davidenko A.O., Galinich V.I. and Mishchenko D.D., Formation of spinel in melt of the MgO-Al_2O_3-SiO_2-CaF_2 system agglomerated welding flux and its effect on viscosity of slag, *The Paton Welding Journal*, **12**, 18-25 **(2012)**

17. Sokolsky V.E., Roik O.S., Davidenko A.O., Kazimirov V.P., Lisnyak V.V., Galinich V.I. and Goncharov I.A.**,** The phase evolution at high-temperature treatment of the oxide-fluoride ceramic flux**,** *Research journal of Chemical Sciences*, **4(4)**, 71-77 **(2014)**

18. Monaghan B.J. and Chen L., Effect of changing slag composition on spinel inclusion dissolution, *Ironmaking and Steelmaking*, **33(4)**, 323-330 **(2006)**

19. Nightingale S.A. and Monaghan B.J., Kinetics of spinel formation and growth during dissolution of MgO in CaO-Al_2O_3-SiO_2 slag, *Metallurgical and Materials Transactions B.*, **39(5)**, 643-648 **(2008)**

20. Coudurier L., Hopkins D.W., Wilkomirsky I., Fundamentals of Metallurgical Processes: International Series on Materials, Fundamentals of Metallurgical Processes, Elsevier Science, Burlington, 417 **(2013)**

21. Albertsson G.J., Effect of the presence of a dispersed phase (solid particles, gas bubbles) on the viscosity of slag, Ms. Thesis, Royal Institute of Technology, Stockholm, Sweden, 27 **(2009)**

22. Frenkel J. Kinetic theory of liquids. Dover, N.Y., 485 **(1968)**

23. Ledovskaya E.G., Gabelkov S.V., Litvinenko L.M., Logvinkov D.S., Mironova A.G., Odeychuk M.A., Poltavtsev N.S. and Tarasov R.V., Low temperature synthesis of magnesium aluminate spinel, *Problems of atomic science and technology*, **38(17)**, 160-162 **(2006)**

24. 24. Sokol'skii V.E. , Kazimirov V.P. and Kuzmenko V.G., X-ray diffraction study of the multi-component oxide systems, *J. Mol. Liquids,* **93(1-3)**, 235-238 **(2001)**

25. Shpak A.P., Sokolsky V.E., Kazimirov V.P., Smyk S., Kunitsky Yu., Structural features of oxide melts system. Academperiodika, Kiev, 137 **(2003)**

26. Kraus W. and Nolze G. Powder cell 3.2, Federal Institute for Materials Research and Testing (BAM), available online at: http://www.ccp14.ac.uk/ccp/web-mirrors/powdcell/a_v/v_1/powder/e_cell.html, (10.01.2012), **(2012)**

27. The Crystallography Open Database (COD), (2009), available online at: http://www.crystallography.net (10.01.2014), **(2014)**

28. JCPDS - International Centre for Diffraction Data, PDF-2 Database ICDD, Release 54, Newton Square, PA, USA, **(2004)**

29. Zevin L.S. and Kimmel G., Quantitative X-ray diffractometry, Springer, N.Y., 300 **(1995)**

30. Lifshin E., X-ray Characterization of Materials, Wiley, Weinheim, 277 **(2008)**

31. Alekseev V.N., Quantitative Analysis: a text book, University Press of the Pacific, Honolulu, 491 **(2000)**

32. Korenman I.M., Methods for quantitative chemical analysis, Khimia, Moscow, 128 **(1989)**

33. Park J.H., Solidification structure of CaO–SiO_2–MgO–Al_2O_3(–CaF_2) systems and computational phase equilibria: crystallization of $MgAl_2O_4$ spinel, *CALPHAD*, **31**, 428-437 **(2007)**

34. Park J.H., Min D.J. and Song H.S. The effect of CaF_2 on the viscosities and structure of CaO-SiO_2(-MgO)-CaF_2 slags, *Metallurgical and Materials Transactions B.*, **33**, 723-729 **(2002)**

35. Nikolaev A.I., Pechenyuk S.I., Semushina Yu.P., Semushin V.V., Kuz'mich L.F., Rogachev D.L.,

Mikhailova N.L., Brusnitsyn Yu.D. and Rybin V.V., Interaction of components of electrode coatings with liquid glass during heating, *Welding International*, **25(5),** 378-381 **(2011)**

36. Sokolsky V.E., Roik A.S., Davidenko A.O., Kazimirov V.P., Lisnyak V.V., Galinich V.I. and Goncharov I.A., X-ray diffraction and SEM/EDX studies on technological evolution of the oxide-fluoride ceramic flux for submerged arc-surfacing, *J. Min. Metall. Sect. B Metall*., **48,** 101-113 **(2012)**